RESEARCH Open Access

Renal transcriptome-wide analyses in association with kidney black carbon load



Leen Rasking¹, Jasper Callemeyn^{2,3}, Congrong Wang¹, Rossella Alfano¹, Michelle Plusquin¹, Maarten Naesens^{2,3}, Tim S. Nawrot^{1,4*} and Katrien De Vusser^{2,3}

Abstract

Rationale and objective Inhaled black carbon (BC) has been previously shown to reach and accumulate in the kidneys. As kidneys filter toxicants, they may be susceptible to adverse effects caused by BC accumulation. We studied gene expressions and pathways related to BC particle load in kidney biopsy tissue.

Study design Gene expression was measured in 29 kidney biopsies performed at one or two years post-transplantation using Affymetrix microarray. We performed a transcriptome-wide association analysis using linear regression analyses, adjusting for individual characteristics to investigate alterations in gene expression in association with kidney BC. Finally, we performed overrepresentation analyses (ConsensusPathDB) to identify enriched pathways and gene ontology sets.

Results The geometric mean (5th, 95th percentile) of BC particle levels was 5.4×10^3 (1.5×10^3 , 4.1×10^4) number of BC particles per mm³ kidney tissue. The BC particle load associated with gene expression in overrepresenting pathways related to ciliopathies, macrophage-derived proteins involved in anti-inflammatory response, DNA damage response, TP53 regulation, and necrosis. We identified BC associated genes involved in GO terms ciliogenesis and ciliary structure, including genes involved in the ciliary plasm and axoneme. Furthermore, we found significantly BC-associated genes involved in RNA-related processes, including e.g., genes in the integrator complex.

Conclusions Here, we identified genes and pathways associated with real-life kidney BC particle load, indicating alterations in gene expression involved in assembly and maintenance of primary cilia, the anti-inflammatory properties of the innate immune system, and DNA damage-related pathways. These findings highlight the need for public health measures to reduce exposure and protect kidney health in at-risk populations.

Keywords Air pollution, Black carbon, Fine particulate matter, Transcriptome, Kidney transplantation, Kidney

*Correspondence:

Tim S. Nawrot

tim.nawrot@uhasselt.be

¹Centre for Environmental Sciences, Hasselt University, Agoralaan Building D, Diepenbeek 3590, Belgium

²Department of Microbiology, Immunology and Transplantation, Nephrology and Renal Transplantation Research Group, KU Leuven, Leuven, Belgium

³Department of Nephrology and Renal Transplantation, University Hospitals Leuven, Leuven, Belgium

⁴Department of Public Health and Primary Care, Environment and Health Unit, Leuven University, Leuven, Belgium



© The Author(s) 2025. **Open Access** This article is licensed under a Creative Commons Attribution-NonCommercial-NoDerivatives 4.0 International License, which permits any non-commercial use, sharing, distribution and reproduction in any medium or format, as long as you give appropriate credit to the original author(s) and the source, provide a link to the Creative Commons licence, and indicate if you modified the licensed material. You do not have permission under this licence to share adapted material derived from this article or parts of it. The images or other third party material in this article are included in the article's Creative Commons licence, unless indicated otherwise in a credit line to the material. If material is not included in the article's Creative Commons licence and your intended use is not permitted by statutory regulation or exceeds the permitted use, you will need to obtain permission directly from the copyright holder. To view a copy of this licence, visit http://creativecommons.org/licenses/by-nc-nd/4.0/.

Introduction

Ambient air pollution is one of the major environmental risk factors to human health, affecting the entire population, and is estimated to cause 4.2 million premature death worldwide each year [1]. This mortality, and most adverse effects observed on human health, are predominantly due to exposure to fine particulate matter, which are particulates with a diameter $\leq 2.5 \, \mu m \, (PM_{2.5}) \, [1, \, 2]$. Exposure to PM_{2.5} has already been indicated as a cause of e.g., adverse cardiovascular events [3-5] and respiratory diseases [6, 7]. A component of PM25 are black carbon (BC) particles, which are derived from the incomplete combustion of e.g., fossil fuels [8]; they have been shown to reach our systemic circulation to spread to distant organs, including the brain [9] and the kidney [10]. Additionally, we have previously shown that in Flanders (Belgium), at low levels of ambient air pollution, BC particles in the urine of healthy children could be traced, mirroring long-term exposure [11].

The human kidneys filter up to 180 L of fluid per day, making them vulnerable to toxic environmental substances, such as BC, which has been shown to reach the kidneys upon inhalation [10]. Previous research already indicated a significant positive association between kidney injury molecule 1, a marker of acute kidney damage, and individualized BC particle load in kidney biopsy tissue [10]. Moreover, higher $PM_{2.5}$ exposure has been associated with increased rates of all-cause mortality, graft failure, and graft rejection in kidney transplant recipients [12, 13].

Research into the effects of PM_{2.5}, and more specifically BC, on gene expression changes in kidney tissue is lacking. Only a limited number of studies have evaluated the genome-wide effect of PM_{2.5} and/or BC [14-17] and were mainly based on peripheral blood samples, other on transplantation cohorts focussing on e.g., tubulointerstitial damage [18], chronic damage [19], or transplant rejection [20, 21], but none focusing on the kidney in relation to air pollution exposure. In other organ systems, such as e.g., the cardiovascular system, research indicated that PM_{2.5} exposure alters the transcriptome of genes that are relevant for heart-associated diseases; identified differentially expressing genes were functionally associated with pathways e.g., related to cardiovascular development, regulation of blood vessel size, vasculature development, and the p53 pathway [22]. The identification of a renal gene expression signature related to BC may provide new insights into the molecular mechanisms underlying the adverse effects of PM_{2.5}, and more importantly BC, exerts on the kidney. Here, we hypothesized that BC not only accumulates in the kidneys, but also causes transcriptomic alterations in kidney tissue, with potential impact on fibrosis progression. Better insight in the downstream pathobiology of pollution-related processes could provide valuable understanding in how air pollution, and more specifically BC, influences human kidney health. To the best of our knowledge, no study so far has investigated the connection between the renal transcriptome and individualized BC exposure.

Materials and methods

Study population

Kidney transplant biopsies were collected within the context of the BIOMArkers of renal Graft Injuries (BIO-MARGIN) and the Reclassification using OmiCs integration in KidnEy Transplantation (ROCKET) study, as described elsewhere [20]. Included post-transplant renal allograft biopsies were collected within the standard of care and routine clinical practice by a trained physician through a percutaneous kidney biopsy according to established medical guidelines. Post-transplant surveillance ("protocol") biopsies are standardly performed at 3, 12, and 24 months after transplantation, in addition to indication biopsies. For this study, all kidney allograft protocol biopsies from single kidney allograft recipients (n = 29) that had transcriptome data and paraffin-embedded kidney biopsy tissue available, which were collected either 12 months (n = 14) or 24 months (n = 15) after kidney transplantation, were included. Each patient only contributed one biopsy. Institutional review boards and national regulatory agencies approved the study protocol at each clinical center (University Hospitals Leuven, Leuven, Belgium; Hannover Medical School, Hanover, Germany; University Hospital Limoges, Limoges, France; and Necker Hospital, Paris, France) [20]. Secondary usage after primary routine care was approved by the ethical committee of the University Hospital of Leuven (S64649).

We extracted comprehensive patient information encompassing patients' sex, age, body mass index (BMI), smoking status, number of days between transplantation, and biopsy sampling from medical records. Smoking status was defined as never, former, and current smoker.

Black carbon detection in kidney biopsy tissue

In the 29 kidney biopsies selected for this study, BC particles that accumulated in kidney tissue as a result of real-life environmental exposure were detected using a specific and sensitive detection technique, based on the non-incandescence-related white light generation of BC particles under femtosecond-pulsed illumination [10, 11, 23, 24]. In brief, 5 tile scans of 3×3 of formalin-fixed paraffin-embedded kidney tissue, sectioned at 4 μ m, were collected at room temperature using a Zeiss LSM880 (Carl Zeiss, Jena, Germany) confocal microscope using a 20x/0.8 M27 (Plan-Apochromat, Carl Zeiss) objective. The confocal microscope is equipped with a two-photon femtosecond-pulsed laser (150 fs, 80 MHz, MaiTai Deep-See, Spectra-Physics, USA) tuned to a central wavelength

of 810 nm with an average 10 mW radiant power at the sample. Captured images were analyzed according to a peak-finding algorithm with MatLab software (2017b, MathWorks, The Netherlands) to count the number of BC particles and with ImageJ free software (Fiji, version 1.53c, USA) to determine the focal volume of each image. BC validation in kidney tissue, using emission fingerprints and fluorescence-lifetime imaging microscopy decay with reference carbonaceous carbon black particles, has been performed previously [10].

Biopsy sample collection and transcriptomic analysis

Biopsy transcriptomic analysis has been described previously [20]. In brief, at least half of one of two needle puncture kidney biopsies was immediately stored in Allprotect Tissue Reagent (Qiagen Benelux BV, Venlo, The Netherlands). Kidney biopsies were stored at 4 °C for a maximum of 72 h before long-term storage at - 20 °C until RNA extraction. Total RNA was isolated using the Allprep DNA/RNA/miRNA Universal kit (Qiagen Benelux BV) on a QIAcube instrument. The quantity and purity of the extracted RNA was measured using Nano-Drop (ND-1000 spectrophotometer, ThermoFisher Scientific, Ghent, Belgium). Additionally, RNA integrity was evaluated using the Eukaryote nano/pico RNA kit (Agilent Technologies, Diegem, Belgium). Subsequently, the extracted RNA was stored at - 80 °C until microarray analysis.

The arrays were washed and stained using streptavidinphycoerythrin on an automated fluidics station (Affymetrix, High Wycombe, UK); arrays were then scanned on the GeneChip Scanner 300 7G system (Affymetrix). Total extracted RNA was amplified and subsequently biotinylated to complementary RNA (cRNA) employing the GeneChip 3' IVT PLUS reagent kit (Affymetrix). Quality of labelled and fragmented cRNA was evaluated with the Agilent 2100 bioanalyzed prior to hybridization to

Table 1 Study population characteristics (n = 29)

Characteristics	Mean ± SD, geometric mean (5th, 95th per- centile), or number (%)
Maternal	
Age, years	51.06 ± 15.16
Women	12 (41.38%)
BMI, kg/m ²	22.54 ± 3.63
Smoking status	
Never	23 (79.31%)
Former	2 (6.90%)
Current	4 (13.79%)
Days between transplantation and biopsy sampling	578.38 ± 192.08
Individualized BC, no. of particles/mm ³	$5.4 \times 10^3 (1.5 \times 10^3,$ $4.1 \times 10^4)$

BC, black carbon; BMI, body mass index

the Affymetrix GeneChip human Genome U133 Plus 2.0 arrays (Affymetrix). This array comprised 54,675 probe sets, covering the whole genome. Furthermore, arrays were washed, stained, and scanned as mentioned above. The resulting image files (.dat files) were generated with the Genechip Command Console software (AGCC) and intensity values for each probe cell (.cel files) were calculated. The microarray data was handled in accordance with the Minimum Information about a Microarray Experiment guidelines. Gene expression data is available at the Gene Expression Omnibus database with the accession number GSE147089.

Statistical analysis

Characteristics of the study population were described as mean (SD), geometric mean (5th, 95th percentile), or number (%). The association between transcript levels of 54,675 probe sets and measured BC particles in kidney biopsy tissue was assessed using univariate and multivariate linear regression models, adjusting for age, sex, BMI, smoking status, number of days between the transplantation and biopsy sampling using R (version 2023.03.0). We adjusted for multiple testing by controlling the Benjamini-Hochberg false discovery rate (FDR) at 5%. FDRadjusted p-values are referred to as q-values. Next, we performed pathway and gene ontology (GO) term analysis, where the genes with an unadjusted p-value < 0.05 of all 54,675 genes were uploaded into the online overrepresentation analysis (ORA) tool ConsensusPathDB (http:// consensuspathdb.org) [25], developed at the Max Planck Institute for Molecular Genetics to identify pathways or GO terms influenced by BC exposure. Pathways with a p-value of < 0.05 were considered significant.

Results

General characteristics of the study population (n = 29)are provided in Table 1. Overall, the average (standard deviation; SD) age was 51.06 (15.16) years, and 41.38% were female. The population's weight was in the normal range, with an average (SD) BMI of 22.54 (3.63), and 79.31% never smoked. The average ± SD number of days between the transplantation and day of biopsy sampling was 578.38 ± 192.08 days. No significant differences were observed in patient characteristics between biopsy sampling after one year or after two years. The geometric mean (5th, 95th percentile) of BC particle levels was 5.4×10^3 (1.5 × 10³, 4.1 × 10⁴) number of BC particles per mm³ kidney tissue. A raincloud plot of the individual BC measurements is shown in Supplemental Fig. 1. There was no significant difference in BC levels between biopsy sampling after one year (n = 14) or after two years (n = 15)(p = 0.85) (Fig. 1).

In the multivariate linear regression model assessing the association between transcript levels and

Rasking et al. Particle and Fibre Toxicology (2025) 22:31 Page 4 of 13

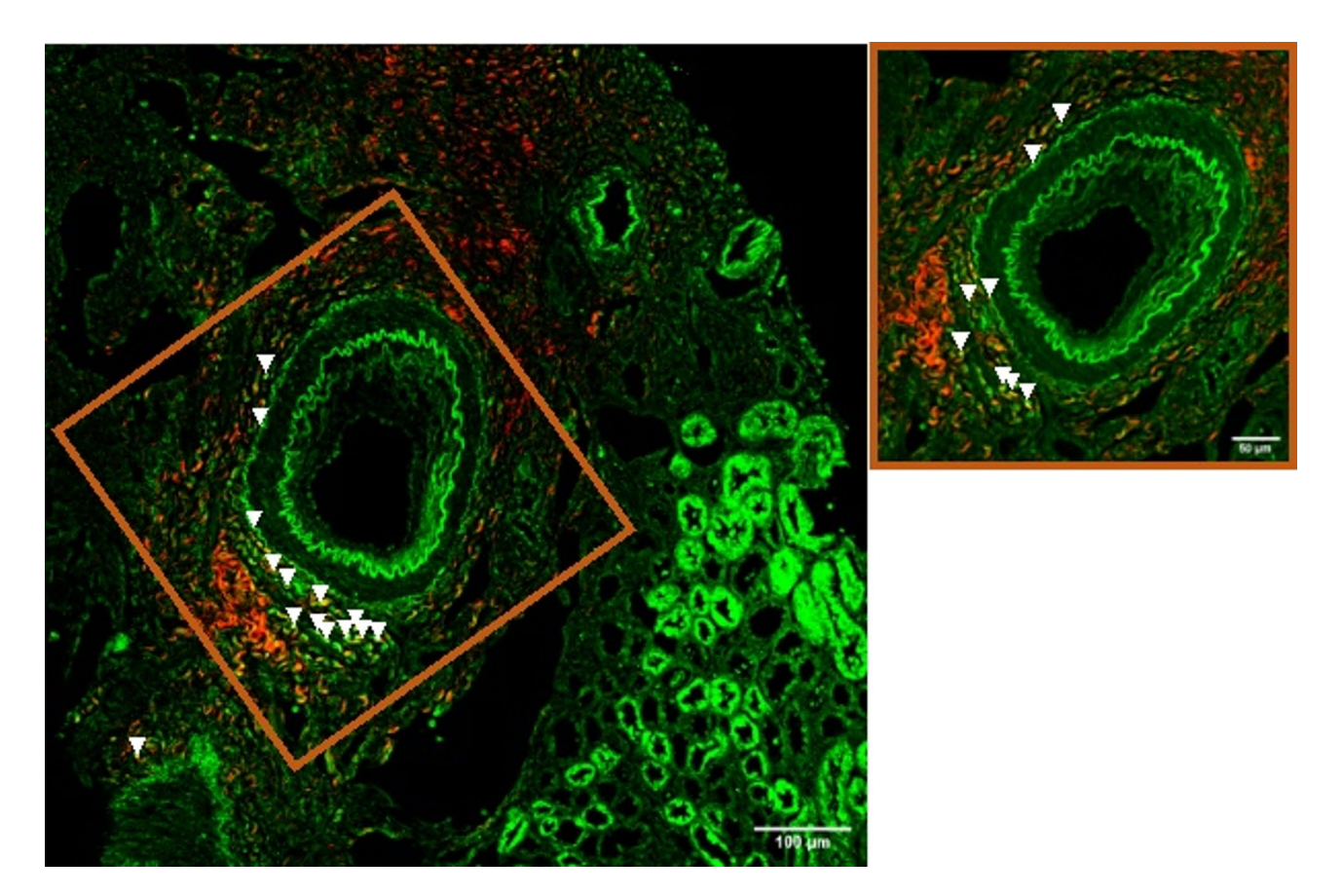


Fig. 1 BC particles in kidney protocol biopsy tissue from a transplant recipient one-year post-transplant. The white light generation which originates from the BC particles (depicted in white and indicated with white arrowheads) under femtosecond-pulsed laser illumination can be observed. Two photon autofluorescence of the tissue (green, em. 450–650 nm) and second harmonic generation from collagen (red, em. 400–410 nm) are detected simultaneously. Scale bar: 100 μm The orange box indicates BC particles present at a higher magnification. Scale bar: 50 μm. *BC* black carbon, *em.* Emission, *ex.* excitation

individualized BC in kidney biopsy tissue, none of the 54,576 genes survived the Benjamini-Hochberg for multiple testing, while 1,318 genes were identified to have a p value < 0.05. Of these 1318 genes, 1010 of them were upregulated and 308 were downregulated. Results are presented by means of a Volcano plot (Supplemental Fig. 2), which depicts the log2 fold change effect size on the x-axis and the significance (without FDR correction) on the y-axis.

Significant effects were further explored by overrepresentation analyses (ORA), which identified 10 significant pathways (Table 2; Fig. 2) and 7 significant GO terms (Table 3). The pathway that comprises ciliopathies, diseases caused by mutations in genes encoding proteins that localize to cilia or centrosomes, was the one with the smallest p value (p < 0.001) associated with individualized BC particle load (Table 2). A more detailed overview of the 18 significant renal genes after ORA, involved in the ciliopathy pathway, is presented in Fig. 3. Here, 10 of the contributing renal-related genes were downregulated, while 8 were upregulated. For example, intraflagellar transport 140 homologue (IFT140) and WD repeat

domain 35 (WDR35), both involved in the formation and maintenance of cilia, were downregulated in relation to individualized BC exposure. Moreover, dynein axonemal heavy chain 11 (DNAH11) and WD repeat containing planar cell polarity effector (WDPCP), both involved in ciliary movement and ciliogenesis, respectively, were upregulated in association to individualized BC particle load. Additionally, other pathways were identified that involve the biosynthesis of maresin and maresin-like specialized proresolving mediators (SPMs) (n = 2), which are critical in the restoration of tissue homeostasis post-inflammation, the DNA damage response (n = 3), regulation of TP53 (n = 2), and necrosis-related pathways (n = 2).

The three significant GO terms with the smallest p values in relation to BC load included 'integrator complex' (p<0.001), of which all genes were upregulated, 'ciliary transition zone' (p<0.001), playing a crucial role in controlling ciliary membrane composition to separate the cytosol from the ciliary plasm, and 'ciliary plasm' (p<0.001), including genes which are important for components of a cilium (Table 3). ConsensusPathDB analyses

Table 2 All significant renal-related pathways associated with BC load after the ORA analysis (n = 10)

Pathway	Effective /total size	Contribut- ing down- regulated genes	Contrib- uting up- regulated genes	p value	q value
Ciliopathies	181/183	TTBK2, FAM161A, CILK1, SPAG1, TRAF3IP1, CEP104, IFT140, GLI2, CEP164, WDR35	DNAH11, TCTN1, PIK3R4, WDPCP, NEK1, DRC1, NEK8, EFHC1	0.0002	0.275
Biosynthesis of maresin-like SPMs	6/6	CYP2E1	CYP3A4, CYP2C9	0.0010	0.399
Biosynthesis of maresins	8/8	CYP2E1	CYP3A4, CYP2C9	0.0027	0.415
DNA damage response	68/68	APAF1, SMC1A, CHEK1	PIDD1, RAD9A, FANCD2, TP53AIP1, RAD52	0.0043	0.512
Regulated necrosis	29/29	IRF2	PELI1, STUB1, RIPK3, FASLG	0.0045	0.512
miRNA regulation of DNA damage response	72/98	APAF1, CHEK1, SMC1A	FANCD2, TP53AIP1, RAD52, RAD9A, PIDD1	0.0061	0.536
Regulation of TP53 activity	160/163	L3MBTL1, CHEK1, GATAD2B, BRIP1,	RAD9A, HIPK2, CHD4, TOP3A, TP53INP1, MAPK11, TAF15, TAF11, BRPF3	0.0085	0.536
Regulation of TP53 activ- ity through phosphorylation	92/93	BRIP1, CHEK1	RAD9A, MAPK11, TOP3A, TP53INP1, TAF15, TAF11, HIPK2	0.0085	0.536
ATM pathway	34/34	SMC1A	TOP3A, RAD9A, FANCD2, SMC3	0.0090	0.536
Regulation of necroptotic cell death	22/22	-	PELI1, STUB1, RIPK3, FASLG	0.0090	0.536

ATM ataxia telangiectasia mutated; SPM specialized proresolving mediators. The effective size represents the number of significant genes (n=1,318) from the input that are found in the respective pathway analyzed. The total size represents the total number of genes in the specific pathway. The q value represents the adjusted p value that control the false discovery rate

revealed other overrepresented GO terms regarding the cilia, such as e.g., axoneme (p = 0.001). Additionally, other GO terms involved in RNA-related biological processes, e.g., 'integrator complex' (p < 0.001), a protein complex mediating the 3'-end processing of RNA, and 'translation activator activity' (p < 0.01), encompassing a group of proteins which have a function in ribosome-mediated translation of mRNA.

Discussion

Population-based studies found that ambient air pollution is associated with a higher risk for the development of chronic kidney disease [2, 12, 26, 27]. Making use of unique data from surveillance (protocol) biopsies one-year and two-year post-transplantation in 29 kidney transplant patients, we identified interesting genes in kidney biopsy tissue that were associated with kidney BC particle load post kidney transplantation. Identified genes belonged to pathways mainly related to renal tubular cilia and associated pathologies, innate immune system-related pathways, such as maresin and maresinlike SPMs, which are macrophage-derived anti-inflammatory molecules, and DNA damage-related processes. We have previously demonstrated direct evidence of BC and related carbonaceous particle translocation in renal structures, where the proximal tubules exhibited the highest relative particle accumulation [28]. Furthermore, in a murine model, we have shown that ultrafine carbonaceous nanoparticle exposure alters tubular and interstitial structures, potentially increasing kidney vulnerability to (environmental) injury [29]. Taken together, these prior observations of tubular accumulation and structural alterations may provide a biological context for the pathways identified in the current study.

Ciliopathies pathway

In our study, we identified multiple cilia-related genes whose expression was significantly associated with individualized kidney BC load, implicating pathways involved in ciliogenesis, intraflagellar transport, and cilium structure. Renal primary cilia are microscopic sensory organelles found on the apical surface of renal epithelial cells in tubular segments [30, 31]. These cilia detect fluid flow across the epithelial layer, initiating a response cascade to maintain the architecture of the nephron and collecting duct [32]. Previously, we showed that tubules are the second most prominent site of BC accumulation in kidney biopsy tissue [10]. In this study, we identified pathways indicating BC-induced changes in ciliogenesis, ciliary trafficking, and cilium structure in the kidney (Fig. 3). Gene mutations affecting ciliogenesis can lead to defects in both cilia structure and function. Persistent cilia dysfunction has been implicated in the early stages and progression of renal diseases [33].

Rasking et al. Particle and Fibre Toxicology

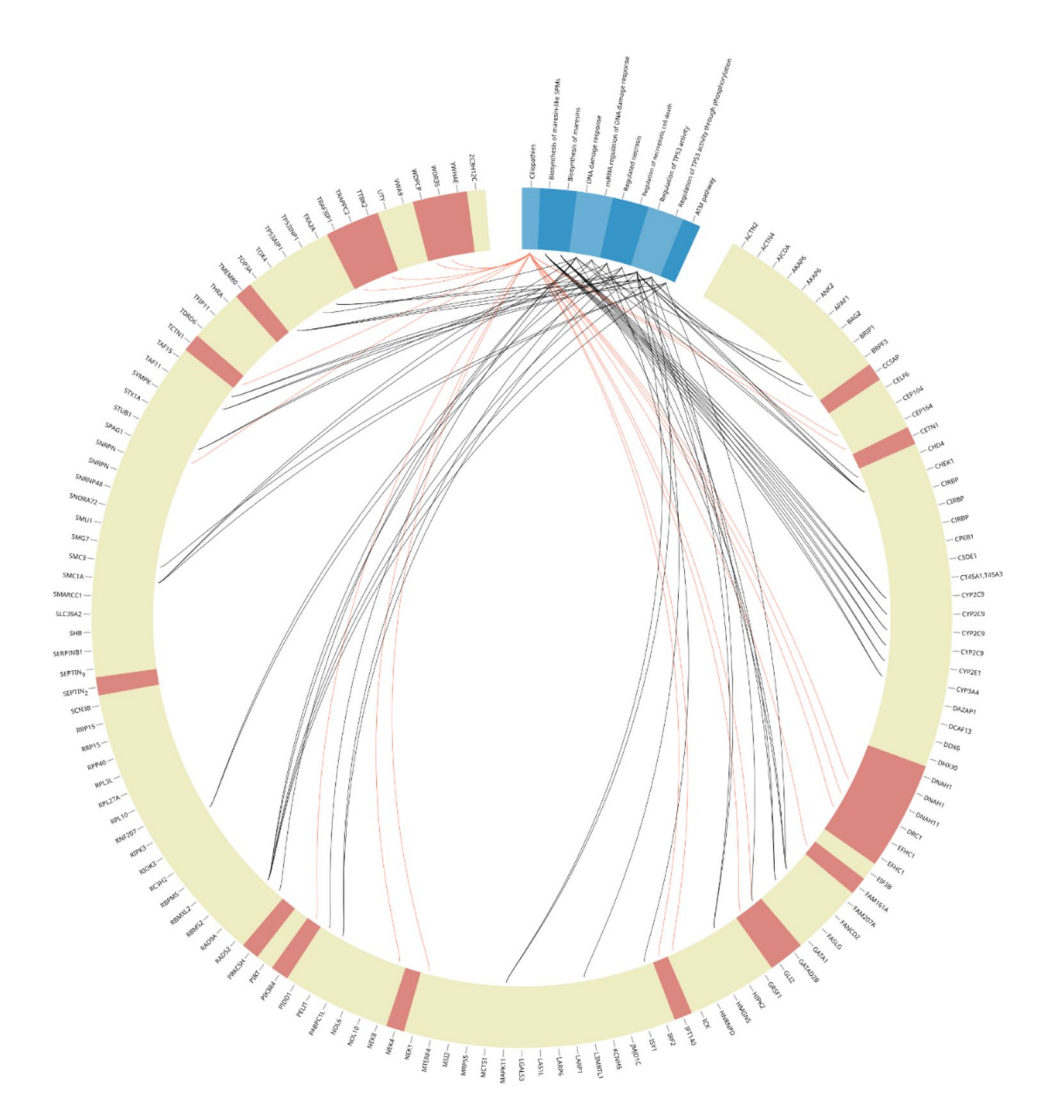


Fig. 2 Schematic overview indicating significantly associated transcripts and their position in identified pathways and GOterms. The ideogram shows the gene transcripts (pale yellow) significantly correlated to identified pathways (blues). Red bands indicate gene transcripts that are involved in the GOterms associated with renal cilia. In the center of the ideogram each significant correlation coefficient is visualized through a link connecting the gene transcript and the identified pathway. Links regarding the ciliopathies pathway are colored red, and other identified pathways are colored black. *ATM* ataxia telangiectasia mutated, *SPM* specialized proresolving mediators

Genes involved in ciliogenesis that were found to be upregulated in association with kidney BC particle load include WDPCP and tectonic family member 1 (TCTN1). WDPCP is essential for the recruitment of proteins in the transition zone [34], while TCTN1 regulates the ciliary membrane composition [35]. Downregulated genes include tau-tubulin kinase 2 (TTBK2), FAM161 centrosomal protein A (FAM161A), and centrosomal protein of 164 kDa (CEP164). CEP164, alongside FAM161A, is a key component of the basal body of the cilium, responsible for recruiting TTBK2 to the mother centriole and triggering ciliogenesis [36]. TTBK2 acts as a negative regulator of ciliogenesis by capping the mother centriole, but is also required for IFT recruitment [36, 37].

The assembly and maintenance of cilia requires intraflagellar transport (IFT), which consists of IFT proteins localized at the base of a cilium [38]. Defects in IFT, as well as in the function of motile or sensory cilia, are associated with numerous adverse kidney outcomes, such as polycystic kidney disease [38]. In this study, genes involved in IFT associated with individualized BC particle load include WDR35, IFT140, and TRAF3 Interacting Protein 1 (TRAF3IP1), all of which were downregulated. The multi-subunit IFT protein complexes consist of IFT subcomplex A (IFT-A) and IFT subcomplex B (IFT-B), supported by Bardet-Biedl syndrome (BBS) proteins and kinesin [39]. IFT-A is essential for the transport of membrane-associated proteins and ion channels, and downregulation of genes involved in the IFT-A subunit, such as IFT140 and WDR35, may result in shortened cilia,

Table 3 Identified gene ontology terms in relation to individualized BC particle load (n=7)

Gene ontology term	Effec- tive/ total size	Contributing downregulated genes	Contributing upregulated genes	<i>p</i> -value	q- value
Integrator complex (GO:0032039)	23/28	-	CT45A1, CT45A2, CT45A3, CT45A5, CT45A6, INTS14	0.00019	0.0181
Ciliary transition (GO:0035869)	67/68	CCSAP, CETN1, SEPTIN2, TCTN1, TMEM80	FAM161A, IFT140, NEK4, TRAF3IP1, TTBK2	0.000242	0.0365
Ciliary plasm (GO:0097014)	129/131	GLI2, IFT140, NEK4, SEPTIN9, TRAF3IP1, WDR35,	CCSAP, DNAH1, DNAH11, DRC1, EFHC1, PIK3R4, SEPTIN2, WDPCP	0.000483	0.0365
lon channel (GO:0044325)	125/129	ACTN4, PRKCSH, TRAPPC2, YWHAE	ACTN2, AKAP6, ANK2, BAG2, KCNH5, PIRT, RNF207, SCN3B, STX1A	0.00113	0.114
Axoneme (GO:0005930)	127/129	GLI2, TRAF3IP1, SEPTIN2, SEPTIN9, WDR35	CCSAP, DNAH1, DNAH11, DRC1, EFHC1, IFT140, PIK3R4, WDPCP	0.00131	0.066
Chromatin DNA binding (GO:0031490)	100/103	ACTN4, GATAD2B, HMGN5, SMARCC1, THRA, TOX4	CHD4, GATA1, JMJD1C, RCC1, UTY	0.00169	0.114
Ribonucleoprotein complex (GO:1990904)	841/878	ACTN4, DCAF13, DDX6, FAM207A, GRSF1, ISY1, LARP1, LARP6, NOL6, NOL10, RBMS2, RC3H2, RIOK3, RRP15, RPP40, SHB, SMU1, ZC3H12C	AICDA, CELF6, CIRBP, CPEB1, CSDE1, DAZAP1, DHC30, EIF3B, HNRNPD, LAS1L, LGALS3, MCTS1, MRPS5, MSI2, MTERF4, PABPC1L, RBMXL2, RBPMS, RPL3L, RPL10, RPL27A, RPL30, SERPINB1, SLC39A2, SMG7, SNRPN, SNRNP48, SYMPK, TRA2A, TDRD6, TFIP11	0.00295	0.14

reducing sensitivity to fluid flow [32, 39]. In contrast, mutations in IFT-B-related genes, such as TRAF3IP1, have been shown to cause ciliogenesis defects [40].

Furthermore, kidney epithelial cells contain a single, non-motile primary cilium; however, motile cilia have also been observed in kidney biopsies [41]. In this study, we found that Sperm Associated Antigen 1 (SPAG1) is downregulated in association with individualized BC particle load. Research indicates that SPAG1 may play a role in the cytoplasmic assembly of the dynein arms of motile cilia [42]. Dynein arms are essential for generating the force required for ciliary beating; here, two genes associated with microtubule-based organelles on the outer dynein arm of motile cilia, DNAH11 and Dynein Regulatory Complex Subunit 1 (DRC1), were upregulated. If cilia are shortened due to downregulation of genes involved in the IFT complex, and a disruption in the cytoplasmic assembly of the dynein arms, compensation in the force of motile cilia may be required [41].

The non-motile primary cilium on the apical side of tubular epithelial cells functions as a fluid flow sensor, regulating tubule diameter based on the urine flow rate [41]. Upregulation of certain genes, such as phosphoinositide-3-kinase regulatory subunit 4 (PIK3R4), may disrupt the IFT's ability to sense fluid flow and respond appropriately [32, 39, 43]. Downregulated genes associated with individualized BC kidney load include never in mitosis A-related kinase 8 (NEK8), which is involved in the regulation of ciliary localization and formation. Adamiok-Ostrowska et al. [44] indicated that downregulation of NEK8 results in the proper maintenance of primary cilia structure. However, ciliopathies

resulting from gene mutations in ciliary proteins often affect not only the kidney but also multiple other organ systems, including the cardiovascular, respiratory, and endocrine systems [45].

Taken together, these results indicate that BC particle load is associated with coordinated changes across multiple components of the cilium, suggesting potential alterations in tubular sensory and motile cilia function.

Inflammatory pathways

In this study, we identified two pathways related to the synthesis of maresin and maresin-like SPMs that were significantly associated with individualized kidney BC load. Maresins are biosynthesized macrophage-derived molecules that help repair and regenerate damaged tissue and clear bacteria and tissue debris [46]. Macrophages play a central role in the acute inflammatory response, with M1 macrophages initiating inflammation and causing tissue damage, while M2 macrophages resolve inflammation by promoting cell proliferation and tissue repair [46, 47]. Moreover, M2 macrophages express higher levels of SPM biosynthetic enzymes, which are crucial for regulating resolution responses. These SPMs counter-regulate the production of inflammation-initiating signals, such as cytokines and chemokines, while also promoting tissue repair and regeneration [46, 48]. In kidney transplantation, M2 macrophage polarization is favorable. Devraj et al. [49] indicated that M2 macrophages dominate in kidney grafts with stable function, whereas M1 macrophages are more prevalent in dysfunctional or rejecting kidney grafts. Additionally, short-term exposure to $PM_{2.5}$ has been shown to promote inflammation [50]. In

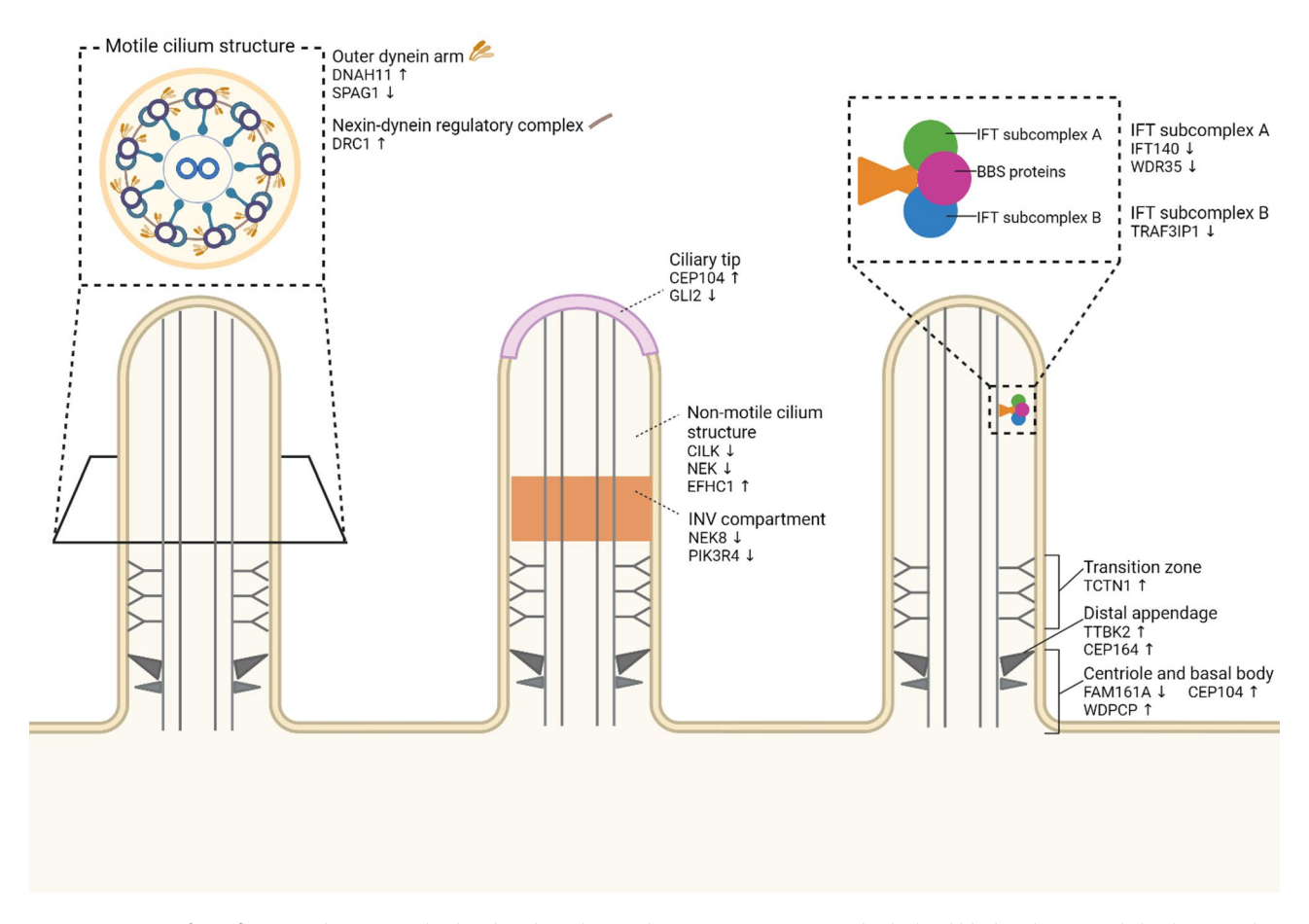


Fig. 3 Overview of significant renal genes involved in the ciliopathies pathway in association to individualized black carbon particle load. *BBS* Bardet-Biedl syndrome, *CEP* centrosomal protein, *CILK* ciliogenesis associated kinase 1, *DNAH11* dynein axonemal heavy chain 11, *DRC1* Dynein Regulatory Complex Subunit 1, *EFHC1* EF-hand domain-containing protein 1, *FAM161A* FAM161 Centrosomal Protein A, *GLI2* zinc finger protein GLI2, *IFT* intraflagellar transport, *NEK8* Never in mitosis A-related kinase 8, *PIK3R4* phosphoinositide 3-kinase regulatory subunit 4, *SPAG1* sperm associated antigen 1, *TCTN1* tectonic family member 1, *TRAF3IP1* TRAF3 interacting protein 1, *TTBK2* tau-tubulin kinase 2, *WDPCP* WD repeat containing planar cell polarity effector, *WDR35* W-D repeat domain. Created with Biorender

chronic obstructive pulmonary disease (COPD) patients, research has shown that $PM_{2.5}$ exposure promotes polarization to M2 macrophages rather than M1 [51]. Similar results were observed when macrophages were exposed to carbon nanomaterials in vitro [52].

The genes involved in the identified maresin pathways associated with individualized BC kidney load were the cytochrome P450 (CYP) monooxygenases CYP2E1, CYP3A4, and CYP2C9, where CYP2E1 was downregulated, while CYP3A4 and CYP2C9 were upregulated (Fig. 4). Maresin biosynthesis is initiated in macrophages by the 14-lipoxygenation of docosahexaenoic acid (DHA), where CYP3A4 and CYP2C9 hydroxylate it to 14*R*-hydroxy-DHA (HDHA). Downregulation of CYP2E1 results in reduced oxidation of 14*R*-HDHA to 14*R*,21*S*/*R*-HDHA [53], which may influence the expression of proinflammatory cytokines and the infiltration of inflammatory cells into the kidney [54]. Additionally, the upregulated CYP3A4 and CYP2C9 are involved in converting the precursor 14*R*-HDHA to the maresin-like

SPM MaR-L2, which has anti-inflammatory properties [55].

Overall, these findings indicate that kidney BC load is associated with coordinated changes in genes driving maresins biosynthesis, highlighting a potential link between particulate exposure and modulation of renal anti-inflammatory pathways.

DNA damage-related pathways

In addition to ciliopathy and maresins pathways, we also identified DNA damage response, regulated necrosis, and TP53 activity pathways that were significantly associated with individualized kidney BC load. The DNA damage response pathway is activated in cells to repair DNA when damage from endogenous or exogenous sources, such as BC exposure, is detected. We have previously demonstrated changes in the methylation and expression of placental and cord blood TP53 genes at birth and linked them to prenatal ambient particulate exposure [56, 57]. In the current study, the most central pathways

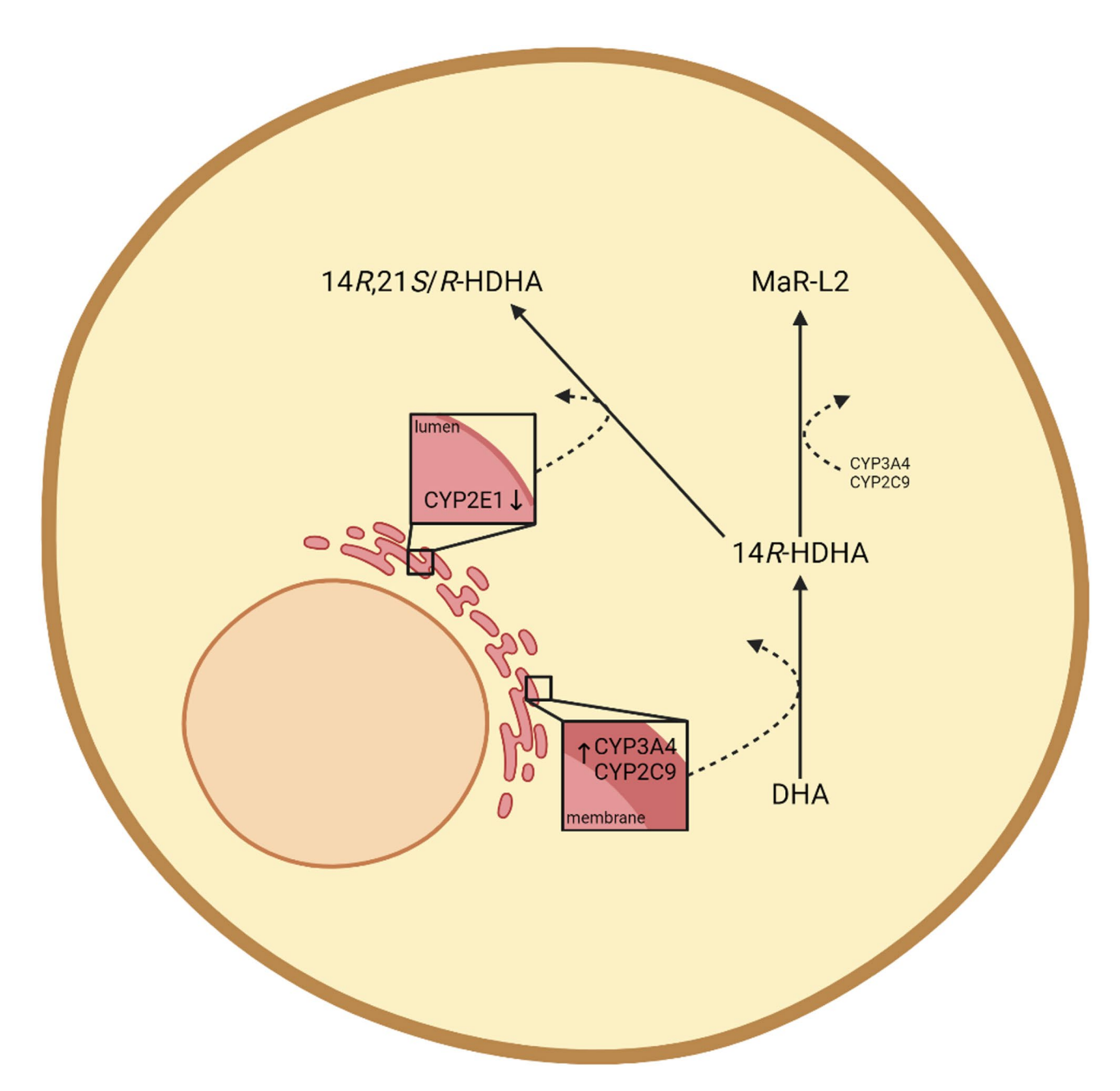


Fig. 4 Simplified schematic overview of the function of BC-associated genes in the maresin biosynthesis pathway. The maresin biosynthesis is initiated in macrophages by the 14-lipoxygenation of docosahexaenoic acid (DHA), where CYP3A4 and CYP2C9, among others, are involved in the hydroxylation to 14R,21S/R-dihydroxy-DHA (HDHA). In a next step, CYP2E1 oxidizes 14R-HDHA to 14R,21S/R-HDHA. 14R-HDHA is a precursor of the maresin-like SPM MaR-L2. *CYP* cytochrome P450, *DHA* docosahexaenoic acid, *HDHA* hydroxydocosahexaenoic acid, *SPM* specialized proresolving mediators. Created with Biorender

in the DNA damage response associated with individualized BC kidney load are the ataxia telangiectasia mutated (ATM) and ataxia telangiectasia and Rad3-related (ATR) pathways. The most crucial genes are TP53 and checkpoint kinase 2 (CHEK2) for ATM and CHEK1 for ATR, respectively [58, 59].

In the ATM pathway (Fig. 5), ATM kinase activates both the downregulated structural maintenance of chromosomes 1 A (SMC1A) and TP53 and the upregulated

Fanconi anaemia group D2 protein (FANCD2). SMC1A is implicated in the cell cycle, where it inhibits growth and enhances apoptosis in various cancers [60–62]. TP53 is involved in the activation of the downregulated TP53AIP1 and P53-Induced Death Domain Protein 1 (PIDD1), both associated with apoptotic cell death induction [63, 64]. PIDD1 activates caspase 8, an upstream regulator of the downregulated APAF1, which is linked to the induction of apoptosis [59]. FANCD2 promotes cell

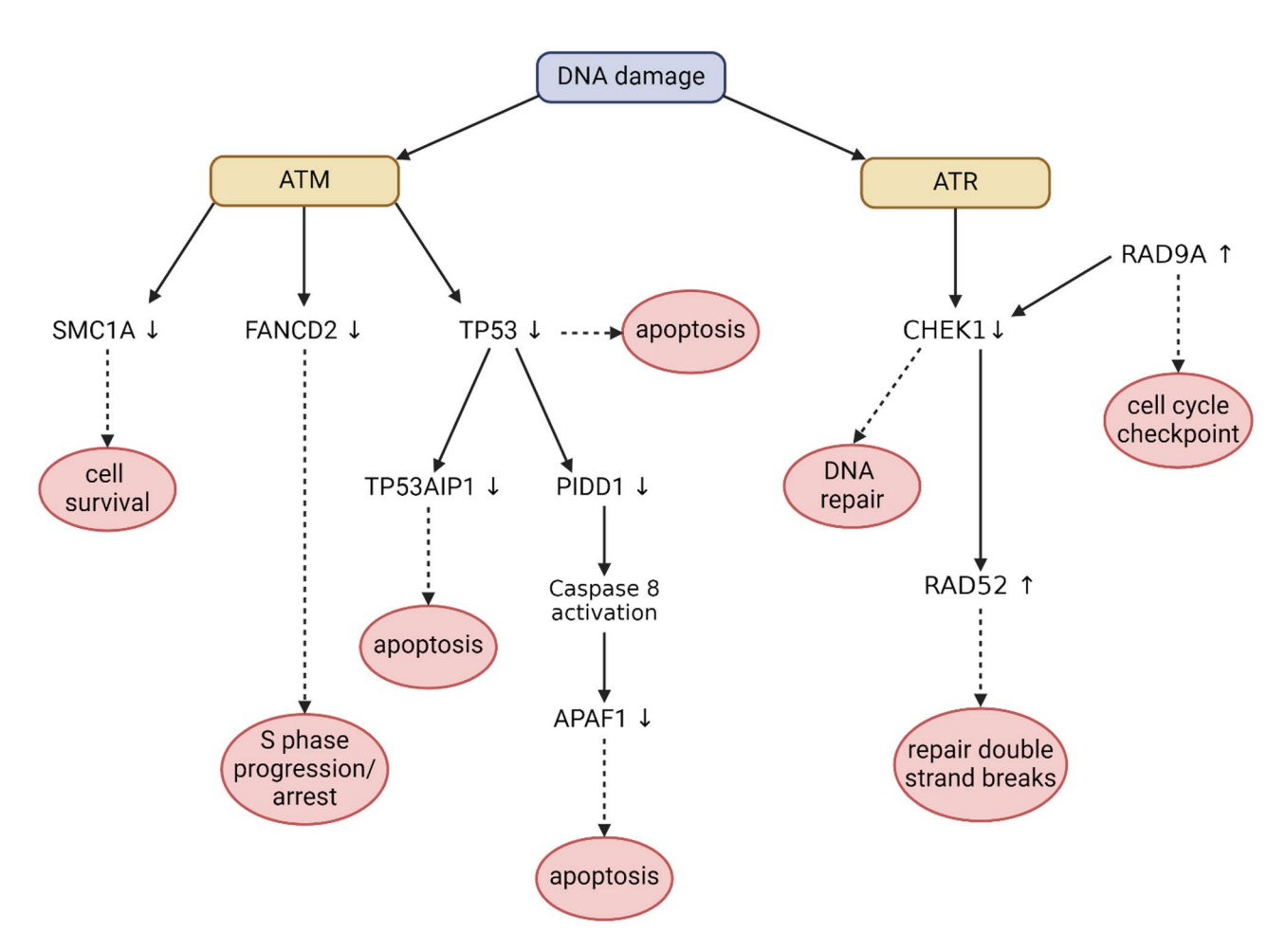


Fig. 5 Simplified schematic overview of the function of BC-associated genes in the ATM and ATR DNA damage pathways. In the ATM pathway, ATM activates the downregulated SCM1A involved in cell survival, FANCD2 involved in cell cycle progression, and TP53 in apoptotic cell death. The latter activates TP53AIP1 and PIDD1, which is found upstream of the downregulated APAF1, which are all involved in apoptotic cell death. In the ATR pathway, ATR, alongside RAD9A, activate the downregulated CHEK1, involved in DNA repair. The upregulated RAD52, involved in the repair of double strand breaks, is activated by CHEK1 upstream. *ATM* ataxia telangiectasia mutated, *APAF1* apoptotic protease activating factor 1, *ATR* ataxia telangiectasia mutated and Rad3-related, *CHEK1* checkpoint kinase 1, *FANCD2* Fanconi anemia group D2 protein, *PIDD1* P53-induced death domain protein 1, *SMC1A* structural maintenance of chromosomes 1 A, *TP53AIP1* p53-regulated apoptosis-inducing protein 1. Created with Biorender

cycle progression by modulating checkpoint proteins to repair DNA damage [65].

In the ATR pathway (Fig. 5), the ATR kinase is activated by DNA double strand breaks and blocks transcription, resulting in the activation of the intra-S checkpoint. ATR, alongside cell cycle checkpoint control protein RAD9A, activates the downregulated CHEK1, which halts cell progression through the S phase. Subsequently, the upregulated RAD52 is downstream activated by CHEK1, playing a crucial role in repairing double-stranded breaks [66]. Overall, the up- and downregulation of the associated genes suggest a tendency toward cell cycle arrest and the promotion of the apoptotic pathway. Synthetic carbon black has previously been shown to induce apoptotic cell death in human lung fibroblasts [67]. It is plausible that BC exposure results in the activation of the apoptotic cell death pathway in the kidney; however, more research is required to elucidate this mechanism.

Lastly, two necrosis-related pathways were identified, where all but one, interferon regulator factor 2 (IRF2), were upregulated. Necroptosis has already been indicated to contribute to acute kidney damage [68]; it is another form of regulated cell death, which depends on the receptor-interacting serine-threonine kinase 3 (RIPK3) [69]. Fas ligand (FASLG) acts as a stimulant for RIPK3 activation [70], which functions upstream in the signal transduction cascade that incites necroptosis [71]. E3 ubiquitin ligase STIP1 homology and U-Box containing protein 1 (STUB1) inhibits necrosis by catalysing the dephosphorylation or ubiquitinylation of RIPK3 [72]. Additionally, PELI1 ubiquitinylates RIPK3, leading to proteasomal degradation of RIPK3 [70].

These observations indicate that kidney BC load is associated with coordinated changes across the DNA damage response, necrosis, and TP53-related pathways,

highlighting potential molecular mechanisms by which BC may affect renal cell homeostasis.

To our knowledge, this is the first study to assess individualized BC particle load from air pollution in association to renal transcriptomics. The individualized BC particle load does not require extensive labelling or sample preparation and was previously established in both kidney tissue and other biological samples [10, 11, 73]. In previous work, we identified the carbonaceous characteristics of the individualized BC particle load in kidney protocol biopsy tissue one-year post-transplant [10]. Nevertheless, our study has some limitations. A limitation of this study is that the BC measured in kidney tissue cannot be traced back to a specific environmental source. BC may derive from various combustion-related sources, including traffic or biomass burning. Our measurements therefore reflect the overall internal BC burden, rather than source-specific exposure. Nevertheless, the biological interpretation remains valid, as the kidney is exposed to BC, regardless of its origin. Additionally, the relatively small sample size limits our ability to account for multiple testing. This reflects a deliberate choice to focus on one- and two-year post-transplant biopsies, which are less affected by transplant-related inflammation or chronic deterioration and thus provide a clearer window on BC-associated molecular changes [74, 75]. Next, we cannot exclude the possibility that some of the BC in the kidneys originates from the donor. However, since we measure BC directly in the kidneys, this should not have significantly biased our results. Furthermore, the study represents a selection of kidney transplant recipients, which may not represent the general population, but might be a selected group which might to be more susceptible to environmental toxicants, such as BC. 10,13 Our findings show that the BC load in kidney tissue is associated with altered gene expression profiles. Due to the observational study design, these data do not allow conclusions on causality. Nonetheless, these observations are consistent with previous studies in both murine and human kidneys [28, 29], which demonstrated that carbonaceous nanoparticles accumulate preferentially in proximal tubules [28] and are associated with alterations in tubular morphology and overall kidney structure [29]. This structural and biodistribution context supports our current observation that BC load is linked to altered gene expression, including in pathway related to cilia and ciliary function.

Conclusion

Exposure to air pollution, more specifically BC, may influence gene expression of primary cilia pathways in renal tubules, potentially contributing to tubular dysfunction through underlying molecular mechanisms. Furthermore, BC may influence gene expression of the innate

immune system pathways, pushing macrophage polarization and contributing to the favoring of apoptotic-related pathways in response to DNA damage caused by BC exposure. With BC particles prominently present in kidney tubules, an interesting avenue for investigation is the impact of BC bioaccumulation on the renal tubules and their cilia, including changes in morphology, histology, and function. Given the critical role of our kidneys in regulating homeostasis of the human body, the identified genes and pathways may reflect molecular mechanisms underlying renal dysfunction associated with BC exposure.

Abbreviations

Abbreviatio	ns
ATM	Ataxia telangiectasia mutated
ATR	Ataxia-telangiectasia mutated and Rad3-related
BBS	Bardet-Biedl syndrome
BC	Black carbon
BMI	Body mass index
CEP	Centrosomal protein
CHEK	Checkpoint kinase
CILK1	Ciliogenesis associated kinase 1
COPD	Chronic obstructive pulmonary disease
CYP	Cytochrome P450
(H)DHA	(hydroxy)docosahexaenoic acid
DNA	Deoxyribonucleic acid
DNAH	Dynein axonemal heavy chain
DRC1	Dynein Regulatory Complex Subunit 1
EFHC1	EF-hand domain-containing protein 1
FAM161A	FAM161 Centrosomal Protein A
FANCD2	Fanconi anemia group D2 protein
FASLG	Fas ligand
FDR	False discovery rate
GLI2	Zinc finger protein GLI2
GO	Genetic ontology
IFT	Intraflagellar transport
NEK8	Never in mitosis A-related kinase 8
ORA	Overrepresentation analysis
PELI1	Pellino E3 Ubiquitin Protein Ligase 1
PIDD1	P53-Induced Death Domain Protein 1
PIK3R4	Phosphoinositide-3-Kinase Regulatory Subunit 4
PM2.5	Fine particulate matter≤2.5 μm
RIPK3	Receptor-interacting serine-threonine kinase 3
RNA	Ribonucleic acid
SD	Standard deviation
SMC1A	Structural maintenance of chromosomes 1 A
SPAG1	Sperm Associated Antigen 1
SPM	Specialized proresolving mediators
STUB1	E3 ubiquitin ligase STIP1 homology and U-Box containing
	protein 1
TCTN1	Tectonic family member 1
TTBK2	Tau-tubulin kinase 2
TRAF3IP1	TRAF3 Interacting Protein 1
WDPCP	WD repeat containing planar cell polarity effector
WDR	W-D repeat domain

Supplementary Information

The online version contains supplementary material available at https://doi.org/10.1186/s12989-025-00646-5.

Supplementary Material 1. Fig. 1. Raincloud plot showing individual black carbon particle levels (log 10-transformed) in kidney biopsies. The half-eye (raincloud) represents the density distribution, the boxplot indicates the median and interquartile range, and the points show individual measurements. Fig. 2. Volcano plot of the transcriptomic analysis for gene expression changes and BC load. The volcano plot shows the difference in

gene expression per log2 fold change in BC load (x-axis) vs. multiple linear regression model p values (y-axis). Multiple linear regression models were adjusted for age, sex, body mass index, smoking status, and the number of days between the transplantation and biopsy sampling. P values < 0.05 are depicted in orange.

Acknowledgements

The authors want to express their greatest gratitude to the kidney transplant patients, as well as the staff of the department of Nephrology at the University Hospitals Leuven.

Author contributions

LR designed and performed the analysis with the help of TSN and KDV. TSN, CW, and JC provided insight into the interpretation of results.JC, MN, and KDV were involved in sample collection, obtaining, and first interpretation of transcriptomic data. LR performed the statistical analysis with help of CW, RA, MP, and TSN. All authors contributed to important intellectual content during manuscript drafting or revision. All authors read and approved the final manuscript.

Funding

LR acknowledges funding from the Special Research Fund (Special Research Fund, BOF) for a doctoral fellowship: BOF20DOC15. The BC work is supported by a Methusalem grant from TSN. The Research Foundation Flanders (FWO) funds JC (1196119 N) and MN (1844019 N). Additionally, MN is supported by an ERAcoSysMed H2020 grant (JTC2_29), and a C3 internal grant from the KU Leuven (C32/17/049). None of the funding agencies had a role in the design and conduct of the study, in the collection, analysis and interpretation of the data, or in the preparation, review, or approval of the manuscript.

Data availability

The data used in the findings of this study are not publicly available as they contain information which may compromise research participant privacy, but are available upon reasonable request from the corresponding author (KDV).

Declarations

Ethics approval and consent to participate

This study was carried out in accordance with the recommendations of the Ethical Committee of UZ Leuven with written informed consent from all subjects. All subjects gave written informed consent in accordance with the Declaration of Helsinki. The study and its secondary usage were approved by the Ethical Committee of UZ Leuven (S64649).

Competing interests

The authors declare no competing interests.

Received: 13 July 2025 / Accepted: 30 September 2025 Published online: 18 November 2025

References

- WHO. Ambient (outdoor) air quality and health. Switzerland: In: WHO Geneva; 2018.
- Kuźma Ł, Małyszko J, Bachórzewska-Gajewska H, Kralisz P, Dobrzycki S. Exposure to air pollution and renal function. Sci Rep. 2021;11(1):11419.
- 3. Hadley MB, Baumgartner J, Vedanthan R. Developing a clinical approach to air pollution and cardiovascular health. Circulation. 2018;137(7):725–42.
- Virani SS, Alonso A, Benjamin EJ, et al. Heart disease and stroke statistics—2020 update: a report from the American heart association. Circulation. 2020;141(9):e139–596.
- Nawrot TS, Perez L, Künzli N, Munters E, Nemery B. Public health importance of triggers of myocardial infarction: a comparative risk assessment. Lancet. 2011;377(9767):732–40.
- Kurt OK, Zhang J, Pinkerton KE. Pulmonary health effects of air pollution. Curr Opin Pulm Med. 2016;22(2):138.
- Nawrot TS, Vos R, Jacobs L, et al. The impact of traffic air pollution on bronchiolitis obliterans syndrome and mortality after lung transplantation. Thorax. 2011;66(9):748–54.

- 8. Janssen NA, Gerlofs-Nijland ME, Lanki T, et al. Health effects of black carbon. World Health Organization. Regional Office for Europe; 2012.
- Vanbrabant K, Van Dam D, Bongaerts E, et al. Accumulation of ambient black carbon particles within key Memory-Related brain regions. JAMA Netw Open. 2024;7(4):e245678–245678.
- Rasking L, Koshy P, Bongaerts E et al. Ambient black carbon reaches the kidneys. Environ Int. 2023:177;107997.
- Saenen ND, Bové H, Steuwe C, et al. Children's urinary environmental carbon load. A novel marker reflecting residential ambient air pollution exposure?
 Am J Respir Crit Care Med. 2017;196(7):873–81.
- Rasking L, Vanbrabant K, Bové H, et al. Adverse effects of fine particulate matter on human kidney functioning: a systematic review. Environ Health. 2022;21(1):1–24.
- 13. Chang S-H, Merzkani M, Murad H, et al. Association of ambient fine particulate matter air pollution with kidney transplant outcomes. JAMA Netw Open. 2021;4(10):e2128190–2128190.
- Espín-Pérez A, Krauskopf J, Chadeau-Hyam M, et al. Short-term transcriptome and MicroRNAs responses to exposure to different air pollutants in two population studies. Environ Pollut. 2018;242:182–90.
- Winckelmans E, Nawrot TS, Tsamou M, et al. Transcriptome-wide analyses indicate mitochondrial responses to particulate air pollution exposure. Environ Health. 2017;16:1–15.
- Croft DP, Burton DS, Nagel DJ, et al. The effect of air pollution on the transcriptomics of the immune response to respiratory infection. Sci Rep. 2021;11(1):19436.
- Rossner P Jr, Tulupova E, Rossnerova A, et al. Reduced gene expression levels after chronic exposure to high concentrations of air pollutants. Mutat Research/Fundamental Mol Mech Mutagen. 2015;780:60–70.
- Vitalone MJ, O'Connell PJ, Wavamunno M, Fung CL-S, Chapman JR, Nankivell BJ. Transcriptome changes of chronic tubulointerstitial damage in early kidney transplantation. Transplantation. 2010;89(5):537–47.
- O'Connell PJ, Zhang W, Menon MC, et al. Biopsy transcriptome expression profiling to identify kidney transplants at risk of chronic injury: a multicentre, prospective study. Lancet. 2016;388(10048):983–93.
- Callemeyn J, Lerut E, de Loor H, et al. Transcriptional changes in kidney allografts with histology of antibody-mediated rejection without anti-HLA donor-specific antibodies. J Am Soc Nephrology: JASN. 2020;31(9):2168.
- 21. Mueller T, Einecke G, Reeve J, et al. Microarray analysis of rejection in human kidney transplants using pathogenesis-based transcript sets. Am J Transplant. 2007;7(12):2712–22.
- 22. Yang X, Feng L, Zhang Y, et al. Integrative analysis of methylome and transcriptome variation of identified cardiac disease-specific genes in human cardiomyocytes after PM2. 5 exposure. Chemosphere. 2018;212:915–26.
- 23. Bongaerts E, Bové H, Ameloot M, Nawrot T. Ambient black carbon particles reach the fetal side of human placenta. Environ Epidemiol. 2019;3:34–5.
- Bové H, Steuwe C, Fron E, et al. Biocompatible label-free detection of carbon black particles by femtosecond pulsed laser microscopy. Nano Lett. 2016;16(5):3173–8.
- Kamburov A, Pentchev K, Galicka H, Wierling C, Lehrach H, Herwig R. ConsensusPathDB: toward a more complete picture of cell biology. Nucleic Acids Res. 2011;39(suppl1):D712–7.
- 26. Chen Y, Cao F, Xiao J-P, et al. Emerging role of air pollution in chronic kidney disease. Environ Sci Pollut Res. 2021;28(38):52610–24.
- 27. Xu X, Nie S, Ding H, Hou FF. Environmental pollution and kidney diseases. Nat Rev Nephrol. 2018;14(5):313–24.
- Rasking L, Vanbrabant K, Vangeneugden M et al. Relative biodistribution and accumulation of carbonaceous nanoparticles inside the murine and human kidney. J Hazard Mater Adv. 2025:19;100790.
- Rasking L, Vanbrabant K, Sun P et al. Kidney morphological changes associated with early-life carbonaceous ultrafine particle exposure: A pathomics approach. Environ Res. 2025;285;122458.
- Deane JA, Verghese E, Martelotto LG, et al. Visualizing renal primary cilia. Nephrology. 2013;18(3):161–8.
- 31. Dell KM. The role of cilia in the pathogenesis of cystic kidney disease. Curr Opin Pediatr. 2015;27(2):212.
- 32. Verghese E, Weidenfeld R, Bertram JF, Ricardo SD, Deane JA. Renal cilia display length alterations following tubular injury and are present early in epithelial repair. Nephrol Dialysis Transplantation. 2008;23(3):834–41.
- 33. Bai Y, Wei C, Li P, et al. Primary cilium in kidney development, function and disease. Front Endocrinol. 2022;13:952055.
- Wasik AA, Dash SN, Lehtonen S. Septins in kidney: A territory little explored. Cytoskeleton. 2019;76(1):154–62.

- 35. Gong S, Ji F, Wang B, Zhang Y, Xu X, Sun M. Tectonic proteins are important players in non-motile ciliopathies. Cell Physiol Biochem. 2018;50(1):398–409.
- Čajánek L, Nigg EA. Cep164 triggers ciliogenesis by recruiting Tau tubulin kinase 2 to the mother centriole. Proc Natl Acad Sci. 2014;111(28):E2841–E2850.
- 37. Liao J-C, Yang TT, Weng RR, Kuo C-T, Chang C-W. TTBK2: a Tau protein kinase beyond Tau phosphorylation. Biomed Res Int. 2015(1):575170.
- Blacque OE, Li C, Inglis PN, et al. The WD repeat-containing protein IFTA-1 is required for retrograde intraflagellar transport. Mol Biol Cell. 2006;17(12):5053–62.
- Jiang M, Palicharla VR, Miller D, et al. Human IFT-A complex structures provide molecular insights into ciliary transport. Cell Res. 2023;33(4):288–98.
- Wang J, Zhu X, Wang Z, Li X, Tao H, Pan J. Assembly and stability of IFT-B complex and its function in BBSome trafficking. Iscience. 2022;25(12):105493.
- 41. Eymael J, Willemsen B, Xu J, et al. Motile cilia on kidney proximal tubular epithelial cells are associated with tubular injury and interstitial fibrosis. Front Cell Dev Biology. 2022;10:765887.
- Knowles MR, Ostrowski LE, Loges NT, et al. Mutations in SPAG1 cause primary ciliary dyskinesia associated with defective outer and inner dynein arms. Am J Hum Genet. 2013;93(4):711–20.
- Stoetzel C, Bär S, De Craene J-O, et al. A mutation in VPS15 (PIK3R4) causes a ciliopathy and affects IFT20 release from the cis-Golgi. Nat Commun. 2016;7(1):13586.
- Adamiok-Ostrowska A, Piekiełko-Witkowska A. Ciliary genes in renal cystic diseases. Cells. 2020;9(4):907.
- McConnachie DJ, Stow JL, Mallett AJ. Ciliopathies and the kidney: a review. Am J Kidney Dis. 2021;77(3):410–9.
- Dalli J, Vlasakov I, Riley IR et al. Maresin conjugates in tissue regeneration biosynthesis enzymes in human macrophages. Proc Natl Acad Sci. 2016;113(43):12232–12237.
- 47. Mills C. M1 and M2 macrophages: oracles of health and disease. Crit Reviews™ Immunol. 2012;32(6):463–488.
- Fullerton JN, Gilroy DW. Resolution of inflammation: a new therapeutic frontier. Nat Rev Drug Discov. 2016;15(8):551–67.
- Devraj VM, Kalidindi K, Guditi S, Uppin M, Taduri G. Macrophage polarization in kidney transplant patients. Transpl Immunol. 2022;75:101717.
- Li X, Cai H, Wu W, Si S, Zhu M. Exposure duration of ambient fine particulate matter determines the polarization of macrophages. Cent Eur J Immunol. 2023;48(1):219–227.
- Jiang Y, Zhao Y, Wang Q, Chen H, Zhou X. Fine particulate matter exposure promotes M2 macrophage polarization through inhibiting histone deacetylase 2 in the pathogenesis of chronic obstructive pulmonary disease. Ann Transl Med. 2020;8(20):1303.
- Kinaret PAS, Scala G, Federico A, Sund J, Greco D. Carbon nanomaterials promote M1/M2 macrophage activation. Small. 2020;16(21):1907609.
- Hajeyah AA, Griffiths WJ, Wang Y, Finch AJ, O'Donnell VB. The biosynthesis of enzymatically oxidized lipids. Front Endocrinol. 2020;11:591819.
- Yamamoto T, Isaka Y. Dietary omega-3 polyunsaturated fatty acids and amelioration of CKD: possible cellular mechanisms. In. Vol 4: LWW; 2023:1661–1662.
- Liu M, He H, Chen L. Protective potential of Maresins in cardiovascular diseases. Front Cardiovasc Med. 2022;9:923413.
- Van Der Stukken C, Nawrot TS, Alfano R, et al. The telomere-mitochondrial axis of aging in newborns. Aging. 2022;14(4):1627.

- Neven KY, Saenen ND, Tarantini L, et al. Placental promoter methylation of DNA repair genes and prenatal exposure to particulate air pollution: an ENVIRONAGE cohort study. Lancet Planet Health. 2018;2(4):e174–83.
- Liu Q, Guntuku S, Cui X-S, et al. Chk1 is an essential kinase that is regulated by Atr and required for the G2/M DNA damage checkpoint. Genes Dev. 2000;14(12):1448–59.
- Cheng Q, Chen J. Mechanism of p53 stabilization by ATM after DNA damage. Cell Cycle (Georgetown Tex). 2010;9(3):472.
- Li J, Feng W, Chen L, He J. Downregulation of SMC1A inhibits growth and increases apoptosis and chemosensitivity of colorectal cancer cells. J Int Med Res. 2016;44(1):67–74.
- Wang J, Yu S, Cui L, et al. Role of SMC1A overexpression as a predictor of poor prognosis in late stage colorectal cancer. BMC Cancer. 2015;15(1):1–11.
- Zhang Y-F, Jiang R, Li J-D, et al. SMC1A knockdown induces growth suppression of human lung adenocarcinoma cells through G1/S cell cycle phase arrest and apoptosis pathways in vitro. Oncol Lett. 2013;5(3):749–55.
- 63. Weiler ES, Szabo TG, Garcia-Carpio I, Villunger A. PIDD1 in cell cycle control, sterile inflammation and cell death. Biochem Soc Trans. 2022;50(2):813–24.
- Oda K, Arakawa H, Tanaka T, et al. p53AIP1, a potential mediator of p53-dependent apoptosis, and its regulation by Ser-46-phosphorylated p53. Cell. 2000:102(6):849–62.
- Nepal M, Che R, Ma C, Zhang J, Fei P. FANCD2 and DNA damage. Int J Mol Sci. 2017;18(8):1804.
- Nogueira A, Fernandes M, Catarino R, Medeiros R. RAD52 functions in homologous recombination and its importance on genomic integrity maintenance and cancer therapy. Cancers. 2019;11(11):1622.
- Bové H, Devoght J, Rasking L, et al. Combustion-derived particles inhibit in vitro human lung fibroblast-mediated matrix remodeling. J Nanobiotechnol. 2018;16:1–12.
- Basile DP, Anderson MD, Sutton TA. Pathophysiology of acute kidney injury. Compr Physiol. 2012;2(2):1303.
- Galluzzi L, Kepp O, Chan FK-M, Kroemer G. Necroptosis: mechanisms and relevance to disease. Annu Rev Pathol. 2017;12:103–30.
- Choi S-W, Park H-H, Kim S, et al. PELI1 selectively targets kinase-active RIP3 for ubiquitylation-dependent proteasomal degradation. Mol Cell. 2018;70(5):920–35. e927.
- 71. Sun L, Wang H, Wang Z, et al. Mixed lineage kinase domain-like protein mediates necrosis signaling downstream of RIP3 kinase. Cell. 2012;148(1):213–27.
- 72. Chen W, Wu J, Li L, et al. Ppm1b negatively regulates necroptosis through dephosphorylating Rip3. Nat Cell Biol. 2015;17(4):434–44.
- 73. Bové H, Bongaerts E, Slenders E, et al. Ambient black carbon particles reach the fetal side of human placenta. Nat Commun. 2019;10(1):3866.
- Nankivell BJ, Fenton-Lee CA, Kuypers DR, et al. Effect of histological damage on long-term kidney transplant outcome. Transplantation. 2001;71(4):515–23.
- Huang Y, Tilea A, Gillespie B, et al. Understanding trends in kidney function 1 year after kidney transplant in the united States. J Am Soc Nephrol. 2017;28(8):2498–510.

Publisher's note

Springer Nature remains neutral with regard to jurisdictional claims in published maps and institutional affiliations.